Dynamics of directional reflectance factor distributions for vegetation canopies

D. S. Kimes

Directional reflectance factors that span the entire exitance hemisphere were measured for vegetation canopies and bare soils with different geometric structures. Two spectral bands were used—NOAA 6/7 AVHRR bands 1 (0.58–0.68 μm) and 2 (0.73–1.1 μm). Geometric measurements of leaf orientation distributions were taken when possible, and other structural and agronomic measurements were collected. For each cover type, these data were taken several different times on a clear day. Polar coordinate system plots of directional reflectance factors, along with 3-D computer graphic plots of scattered flux, were created. These field data were used in conjunction with literature data to study the dynamics of the directional reflectance factor distribution as a function of the geometric structure of the scene, solar zenith angle, and optical properties of the leaves and soil. Physical mechanisms causing the observed dynamics were proposed and were supported by a number of field and modeling studies. For complete homogeneous vegetation canopies, the major trend observed at all sun angles and spectral bands was a minimum reflectance near nadir and increasing reflectance with increasing off-nadir view angle for all azimuth directions. This trend is well known in the experimental and theoretical literature and is caused by the shading of lower canopy layers by components in the upper layers and by viewing different proportions of the layer components as the sensor view angle changes. In some cases the reflectance minimum was shifted slightly off-nadir in the foward scattering direction. The reflectance distributions tended to be azimuthally symmetric because the leaf transmittance was nearly equal to the leaf reflectance for most wavelengths. For sparse homogeneous canopies the anisotropic scattering properties of the soil significantly influenced the observed directional reflectance in the visible band. Soils have strong backscattering characteristics which can dominate the observed reflectance distribution for sparse canopies and small solar zenith angles. This knowledge is important in interpreting aircraft and satellite data, where the scan angle varies widely and can have different orientations with respect to the sun. Finally, the measured data and knowledge of the mechanics of the observed dynamics of the data can provide rigorous validation and verification tests for theoretical radiative transfer models.

I. Introduction

Few directional reflectance factor measurements which cover the entire exitance hemisphere of natural vegetation and soil scenes have been published. These measurements are needed to understand the directional scattering properties of natural surfaces as a function of the optical properties and geometric structure of the scene components (leaves, stems, reproductive structures, and soil) and the anisotropic distribution of sky radiance.[1] This knowledge can be used to improve the interpretation of remote-sensing data acquired from aircraft and satellite, where the scan angle varies widely and can have different orientations with respect to the sun.[2] For example, the advanced very high resolution radiometer (AVHRR) data from the NOAA satellites offer the potential of monitoring terrestrial targets with a high temporal frequency for large global areas.[3] However, these data are acquired by the radiometer scanning out to 56° from nadir in the plane normal to the satellite's swath path. Even the potential development of pointable earth-observation satellite sensors, while providing the opportunity to improve the temporal resolution of a scene by looking across adjacent swaths, requires better understanding of the effects of viewing various targets off-nadir.[4] Directional measurements that cover the entire exitance hemisphere also serve as rigorous validation data for theoretical radiative transfer models.[5]

In this study, directional reflectance factors which spanned the entire exitance hemisphere were collected on the ground for a variety of homogeneous vegetation canopies and bare soils. NOAA 6/7 AVHRR bands 1 (0.58–0.68 μm) and 2 (0.73–1.1 μm) were used. Simultaneously with each spectral measurement, geometric measurements of leaf orientation distributions were taken when possible. Other supporting structural

The author is with NASA Goddard Space Flight Center, Earth Resources Branch, Greenbelt, Maryland 20771.

Received 3 January 1983.

and optical measurements were taken. These data sets were taken at various times of the day for each cover type. These unique data sets and pertinent data in the literature were used to study the dynamics of the directional reflectance factor distribution as a function of the geometric structure of the scene, solar zenith angle, and optical properties of the scene components (leaves and soil).

II. Experiment

Spectral directional radiances were taken in NOAA satellite 6/7 AVHRR bands 1 (0.58–0.68 μm) and 2 (0.73–1.1 μm) using a Mark III three-band radiometer with a restricted 12° field of view. For each measurement period, forty-one directions were measured located at nadir and at 15° increments of off-nadir angle (15, 30, 45, 60, and 75°) and 45° increments of azimuth angle (0, 45, 90, 135, 180, 225, 270, and 315°). The 0° azimuth corresponds to the direction of the sensor looking toward the sun. Thus, an azimuth of 0 and 180° represents forward scattering and backscattering, respectively. The coordinate system used is shown in Fig. 1.

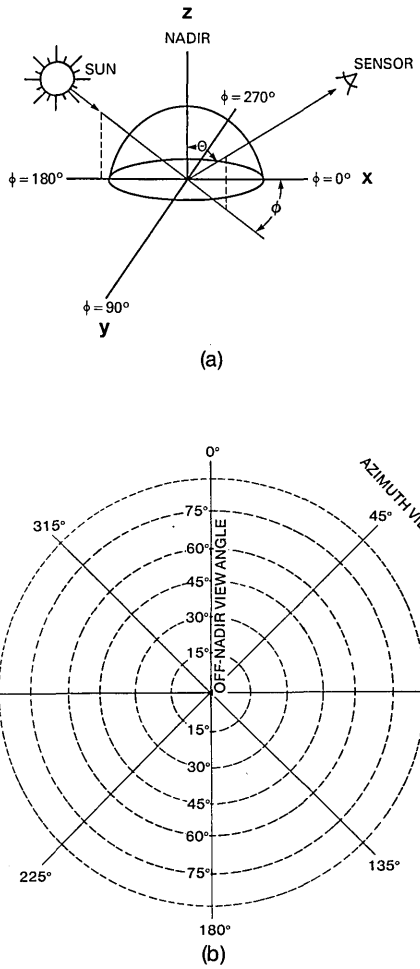

Fig. 1. (a) Coordinate system defining solar and sensor angles and (b) polar plot showing scheme for plotting directional reflectance factors. The solar azimuth is always 180°. The sensors azimuth and off-nadir angles are shown as ϕ and θ, respectively. A sensor with a 0° azimuth looks into the sun. Thus, an azimuth of 0 and 180° represents forward scattering and backscattering, respectively. The spectral directional reflectance factors were plotted in a polar plot, where the distance from the origin represents the off-nadir view angle of the sensor and the angle from ϕ = 0° represents the sensor's azimuth. The points show the directional measurements plotted. Lines of equal reflectance were contoured as presented in Fig. 3.

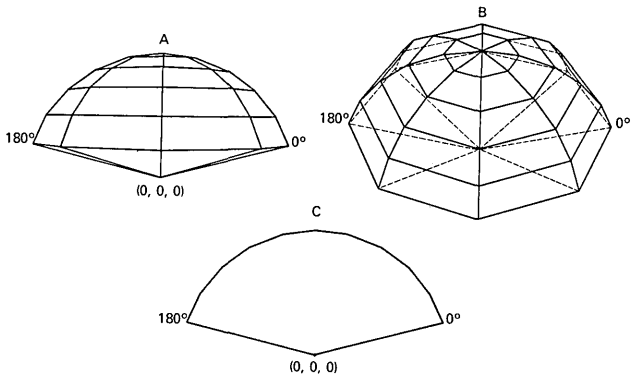

Fig. 2. Three-dimensional plots of a directional reflectance factor distribution of a Lambertian surface with directional intervals as used in this study. The coordinate system used is presented in Fig. 1. The length of any vector as measured from the origin to the surface of the distribution represents the relative magnitude of reflectance factor in the direction of that vector. The three plots are different views: (A) A horizontal view of the X-Z plane, where the X axis is the 0° azimuth, (B) a 45° rotation of view A about the X axis, and (c) a cross section of the principal plane of the sun, which is the X-Z plane. Note that, in the context of the study, an off-nadir view angle of 90° was not measured; thus in all 3-D plots the first data point occurs at 75° off nadir.

For each measurement period, four complete directional radiance distributions were taken at different sampling points within the middle of a homogeneous surface. This sampling procedure took <20 min. One mean distribution was calculated for each measurement period. All mean directional values were divided by the corrected total global irradiance divided by π as obtained from a barium sulfate panel. The resulting values are reflectance factors.[1] The corrected total global irradiance refers to corrections made for the non-Lambertian behavior of a reference panel for the specific irradiance conditions as described by Kimes and Kirchner.[6] For these corrections the distribution of diffuse sky radiance was taken from the simulated data sets of Dave.[7]

The method of plotting the directional reflectance factor distributions is described in Fig. 1. In addition, a 3-D surface of selected directional reflectance factor distributions was created using the graphic package MOVIE.[8] The 3-D surfaces are explained in Fig. 2.

The radiometric data were collected for various surface types and solar zenith angles as reported in Table I. The radiometric measurements of the orchard grass were taken at a height of 3.5 m above the ground, and all other surfaces were measured at 1.5 m. The agronomic characteristics of the vegetation canopies and the spectral reflectance of scene components (leaves and

Table I. Date, Standard Time, and Solar Zenith Angle of Directional Radiometric Measurements of Surface Types

Surface type	Date	Standard time	Solar zenith angle (deg)
Grass lawn (*Festuca abundinacea* Schreb.)	6/9/82	0645	70
		0750	56
		0900	42
Soybeans (*Glycine max* L.)	8/19/82	0640	76
		0751	63
		1007	49
		1132	28
Corn (*Zea mays* L.)	6/2/82	0650	68
		0845	46
		1035	23
Orchard grass (*Dactylis glomerata* L.)	9/17/82	0640	82
		0735	71
		0845	58
		1002	45
Avondale loam soil	6/28/82	0600	82
		0740	63
		0946	37
		1045	24

III. Results and Discussion

Table I presents the dates, time, and solar zenith angles of the radiometric measurements. The agronomic characteristics of the vegetation canopies and the spectral reflectance of scene components (leaves and soil) are presented in Table II. The leaf orientation distributions are presented in the Appendix and are required information for current radiant transfer models. These leaf orientation distributions are a primary factor in determining the probability of gap through the canopy as a function of viewing angle. This is discussed further in Sec. III.A.

The dynamics of reflectance factor distributions can be divided into four categories according to spectral band and whether the vegetation canopy is complete or sparse. In a complete canopy the ground is almost or totally covered by vegetation in the vertical projection. A sparse canopy varies from essentially bare soil to complete canopy cover.

A. Visible Band—Complete Canopy Cover

Figures 3–5 show the reflectance distributions in the visible band (AVHRR band 1) of the relatively complete grass lawn and soybean canopies. In the visible band

Table II. Agronomic Characteristics of Vegetation Canopies; Typical Values of the Hemispherical Reflectance of the Leaves and Nadir Reflectance Factor of Soil are Shown for the Visible and IR Bands

Cover	Date	Height (cm)	Percent cover	Wet biomass g/m^2	Dry biomass g/m^2	Leaf area[c] index	Visual % chlorosis	Leaf reflect.[b] visible (IR)	Leaf trans.[b] visible (IR)	Soil reflect.[d] visible (IR)
Corn[a]	6/02/82	33	25	350	—	0.65	0–5	0.073 (0.38)	0.063 (0.55)	0.18 0.23
Lawn	6/09/82	14	97	—	480	9.9	0–5	—	—	—
Soybeans	8/19/82	77	90	1375	375	4.6	0–5	0.065 (0.43)	0.055 (0.48)	—
Orchard Grass	9/19/82	22	50	413	197	1.1	30–40	—	—	0.18 (0.30)

[a] Corn was randomly planted for a relatively uniform canopy with no row effects.
[b] From Beckman DK-2A spectral reflectometer measurements of laboratory plants weighed by the spectral response curve of the AVHRR bands.
[c] Derived from knowledge of percent cover and approximate leaf angle distribution.
[d] Soil reflectance is the mean *in situ* nadir reflectance of sunlit soil for all solar zenith angles.

soil) are presented in Table II. For details on how these measurements were made, see Kirchner *et al.*[2] In addition, a field of bare Avondale loam soil was measured in Phoenix, Ariz. on 28 June 1982. The soil surface was a smooth surface compacted by rain. All measurements were taken under clear sky conditions.

The 3-D orientation of leaves described as a leaf inclintion-azimuth angle distribution plotted in polar coordinates was measured throughout the morning period for the soybean and corn canopies. The measurements are described by Kimes and Kirchner[9] and show the orientation of the leaves, which are the primary scattering units of the canopy. For the soybean canopy, the orientation of individual leaflets treated as finite planes was measured. In the corn canopy, the orientation of 6-cm leaf segments along the entire length of a leaf was measured and treated as finite planets.

the leaves are highly absorptive, and thus for complete canopies the soil has little effect on the sensor signal. The dynamics of the distributions are as follows.

In general, for complete, homogeneous, vegetation canopies the directional reflectance factor increases as the off-nadir view angle increases for all azimuth view angles and sun angles. This trend is well known in the experimental and theoretical literature[2,10–15] and is caused by the shading of lower canopy layers by the components in the upper layers and by viewing different proportions of the layer components as the sensor view angle changes (Fig. 6). This phenomenon is termed Effect 1 throughout the paper. The underlying principles are stated more rigorously as follows.

If we consider any abstract homogeneous canopy with multiple layers of equal leaf geometry, density, and optical properties, the probability of gap to any par-

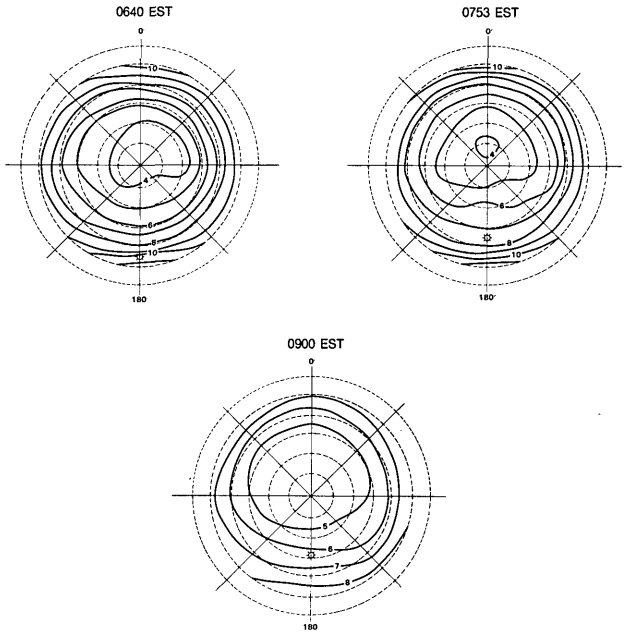

Fig. 3. Polar plots of the directional reflectance (%) in the visible band for the grass lawn. The polar coordinate system is described in Fig. 1. Solar position is shown as a small starred circle on each plot, and standard time is also indicated.

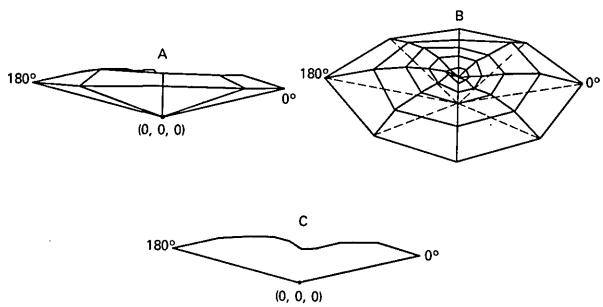

Fig. 4. Three-dimensional plots of the directional reflectance in the visible band for the grass lawn at 0645 (EST). The different views are described in Fig. 2.

ticular canopy depth generally decreases as the off-nadir angle of view increases. Furthermore, for any particular view direction the probability of gap decreases with increasing depth into the canopy. These phenomena are a direct result of the canopy's geometric structure.[15] For all irradiance conditions, this structure causes the scattered solar flux from the components to be maximum at the top of the canopy and decrease to a minimum at the bottom of the canopy. The exact distribution of flux is a complex function of the geometric structure, optical properties of the components, and anisotropic distribution of solar irradiance and has been modeled by many individuals as presented by Smith and Ranson.[16] It is also clear that this structure causes the proportion of components viewed at any given depth (or layer) to decrease with increasing off-nadir view angle. Thus, the ultimate result is that the reflectance increases with increasing off-nadir view angle because, in the sensor's field of view, the proportion of upper canopy components that scatter the largest amount of solar flux increases and the proportion of lower canopy components that scatter the lowest amount of solar flux decreases. It follows that the minimum reflectance should occur near nadir. Finally, the increase of reflectance with increasing off-nadir view angle should be the greatest when the sun is near the horizon and should be minimal when the sun is near the zenith.

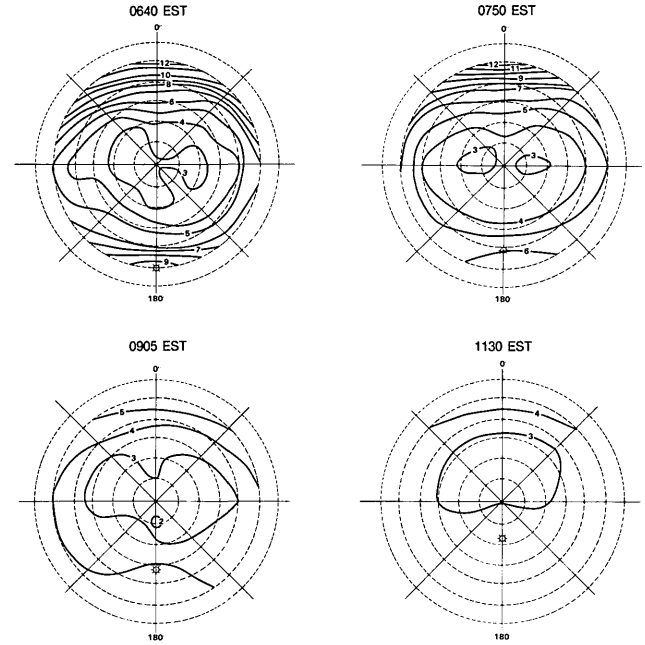

Fig. 5. Polar plots of the directional reflectance (%) in the visible band for the soybeans. Symbols follow Fig. 3.

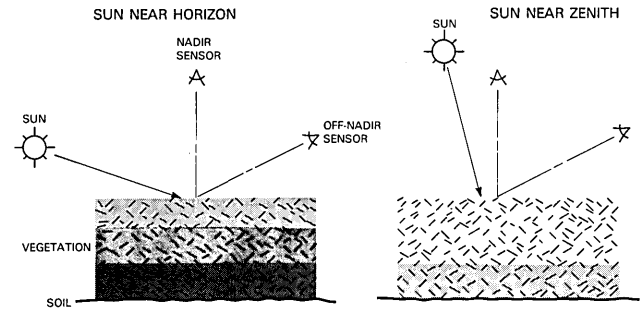

Fig. 6. Effects of sun and view angles on dirfectional reflectance factors of complete vegetation canopies. Shading shows the relative degree that the components of various layers intercept and scatter solar flux. Dark shading is low interception and scattering, and light shading is high. The gradiate of interception and scattering as a function of canopy layers is greatest when the sun is near the horizon. In general, for all homogeneous, complete canopies and for all sun angles, the directional reflectance factor increases as the off-nadir view angle increases for any azimuth view direction. This phenomenon is referred to as Effect 1 in the text. It is caused by the shading of lower canopy layers by the components in the upper layers and by viewing different proportions of the layer components as the sensor view angle changes.

In many canopies the minimum reflectance occurs slightly toward the forward scatter direction—i.e., off-nadir in the 0° azimuth direction[2,11,14] (Fig. 3, 0730 EST, 0900 EST; Fig. 5, 1130 EST). It may be that, in this view direction, the sensor views a higher proportion of the shaded sides of vegetation components[17] which are not exposed to direct solar radiation. If this was the only mechanism operating, one would expect the reflectance in the forward scattering direction to continually drop with increasing off-nadir view angle. However, the minimum reflectance occurs only slightly off nadir (<30°) because Effect 1 becomes dominant at steeper off-nadir view angles.

This shift of minimum reflectance to off nadir in the forward scattering direction seems to occur at more moderate solar zenith angles, e.g., <55°. This can be explained by the fact that, at moderate sun angles, the distribution of intercepted solar flux as a function of height within the canopy is more uniform than with sun angles near the horizon (Fig. 3). Thus, Effect 1 is greatly diminished within the 0–30° off-nadir angle range, and the second effect of decreasing reflectance with increasing off-nadir angle is apparent. Effect 1 quickly dominates at the steeper view angles. Following this logic one would expect that the denser the canopy, the less likely that a shift would be apparent, since Effect 1 would increase. Perhaps this explains why the dense lawn (Fig. 3) shows a minimal shift. Furthermore, one would expect that the higher the leaf transmittance, the less likely that a shift would be apparent, since the backside of leaves would be brighter.[17]

If only Effect 1 were operating and all radiant interactions with canopy components were isotropic, the 3-D reflectance distribution would be an azimuthally symmetric bowl with the center at the origin.[5] The curvature and steepness of the side of the bowl would be a function of the leaf inclination distribution, leaf density, scattering coefficient of leaves and soil, and the anisotropic distribution of solar radiance. However, in addition to Effect 1, we observe the backshadow effect of canopy components as mentioned above and forward scattering and backscattering mechanisms. In general, forward scattering occurs on relatively level surfaces, while backscattering occurs on surfaces which have a vertical structure. For example, when canopy components are Lambertian and horizontal, no azimuthal variation in reflectance will result. However, in reality, some specular reflection may occur, resulting in forward scattering. In addition, essentially all natural scenes have some vertical components. All components scatter flux by reflection or transmission. A scene with opaque vertical components should show large azimuthal variations[10,17] because the front surface (toward the sun) should reflect flux toward the sun both specularly and diffusely and the back surface should be shaded. Furthermore, the component will shade other components within its shadows. The more opaque the components, the darker the shadows. Thus the peak reflectance will occur toward the sun (180° azimuth), and reflectance will decrease in any direction from this direction because the contribution of shadows will increase. For example, soils have vertical components which have very low transmittance, and thus dark shadowing of scene components occurs (Fig. 7). In the antisolar direction (backscatter toward the sun) only those surfaces which are in direct sunlight are viewed by the sensor, and thus the reflectance is maximum in this direction. As the sensor direction moves away from the antisolar direction, the following two mechanisms cause the reflectance to decrease. (1) In the sensor's field of view the relative proportion of shadowed surfaces increases. (2) In the sensor's field of view the proportion of particle facets with normals that deviate from the solar direction increase, causing decreased solar irradiance on these facets (cosine function). These trends are shown in Fig. 12 and are supported by Refs. 10 and 11. In complete vegetation canopies we do not tend to see such extreme azimuthal variation because the transmittance nearly equals the reflectance of leaves in the visible region.[17] Thus, the drastic difference between backscattering and forward scattering characteristics of soils is not observed for vegetation canopies (Fig. 7).

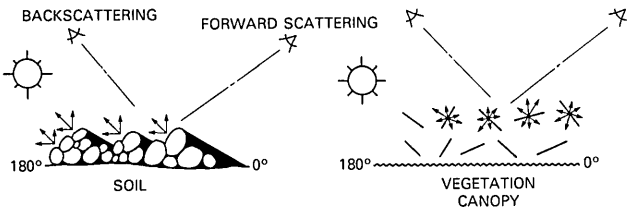

Figure 7. Forward scattering and backscattering of soil and vegetation. Soil generally exhibits strong backscatter and weak forward scatter because of the vertical components and opacity of the components. In contrast, complete vegetation canopies do not exhibit these extreme azimuthal variations because of the transmittance and reflectance of the components (leaves) are relatively equal.

B. Visible Band—Sparse Canopy Cover

Sparse canopies show greater variability in directional reflectance with changing solar zenith angles as opposed to complete canopies. In general, sparse canopies exhibit a strong backscattering toward the sun (antisolar direction). This backscatter peak is most pronounced for very low vegetation cover and diminishes as the canopy approaches complete cover (Fig. 8).[2,14] However, for large solar zenith angles the reflectance distribution is similar to the distribution for complete canopies (Fig. 8, 0655 EST; Fig. 9, 0640 EST). An explanation of these trends is as follows.

For sparse canopies the scattering properties of the soil significantly influence the directional reflectance. In general, the soil hemispherical reflectance is much higher than the leaf reflectance in the visible band. Furthermore, soils generally show strong backscattering for all solar zenith angles. Thus, for moderate-to-small solar zenith angles the soil intercepts and scatters a large proportion of direct solar irradiance, which causes a

strong backscattering peak to occur. The peak is relatively unobscured by vegetation at relatively small solar zenith angles. In any view direction away from this peak the reflectance decreases because of the two soil mechanisms discussed previously. In addition, at off-nadir view angles which are greater than that of the peak backscatter, the reflectance decreases even more since the sensor views a higher proportion of leaf material, which is lower in reflectance than the soil. At large solar zenith angles, however, the solar flux reaching the soil is insignificant, and thus the reflectance distribution looks more similar to a complete canopy (Fig. 8, 0655 EST; Fig. 9, 0640 EST).

These are the trends one would expect for sparse vegetation cover (<30%). However, as vegetation density increases we would expect to see transitional distributions between sparse and complete canopies. For example, Figs. 9–11 shows orchard grass with 50% plant cover. At 0640 EST the sun is near the horizon and the reflectance distribution looks similar to a complete canopy. However, as the sun rises a stronger soil backscatter peak toward the sun is apparent because a greater portion of the direct solar flux reaches the soil and also a high proportion of the soil is viewed in the antisolar direction. At the higher sun angles the minimum reflectance occurs in the forward scatter (0° azimuth) direction. Several mechanisms are operating which determine the position of this minimum: (1) the vegetation density is great enough to cause a significant amount of shadowing in the forward scattering direction, (2) as the off-nadir viewing angle increases in the forward scattering direction, the directional reflectance of the soil drops and the proportion of the low reflecting

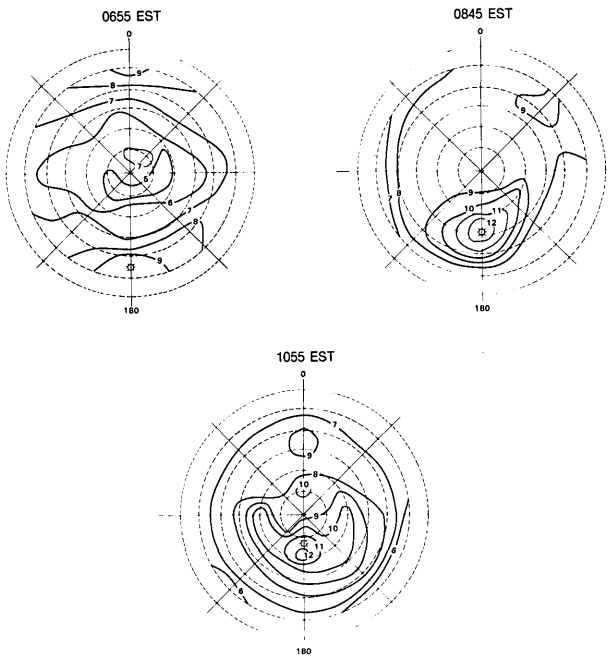

Figure 8. Polar plots of the directional reflectance (%) in the visible band for the corn. Symbols follow Fig. 3.

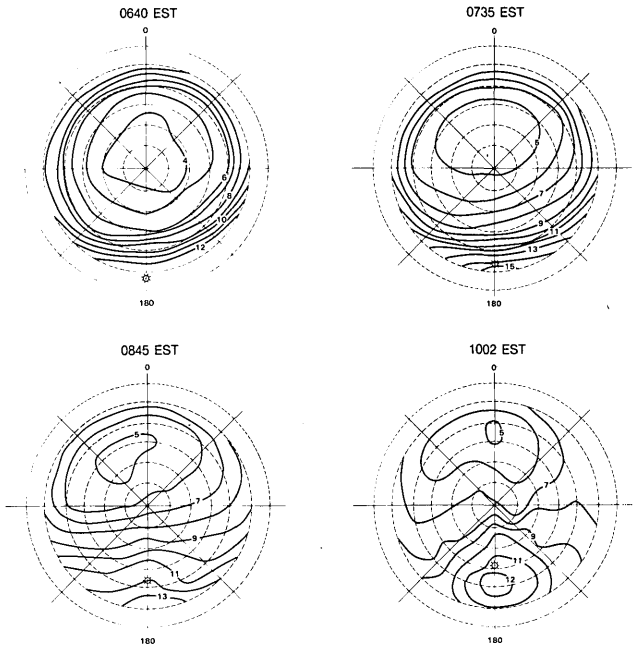

Figure 9. Polar plots of the directional reflectance (%) in the visible band for the orchard grass. Symbols follow Fig. 3.

vegetation (relative to soil) viewed increases, and (3) at some large off-nadir view angle the sensor views only vegetation, and at off-nadir angles greater than this the reflectance increases due to Effect 1 dominating all other mechanisms. Kirchner *et al.*[2] show similar trends for an alfalfa canopy with 42% cover. Another similar pot for a grassland is presented by Salomonson and Marlatt.[18]

As the sun rises, the minimum reflectance moves away from nadir (Fig. 9) because the magnitude of Effect 1 decreases. As the density of vegetation increases, Effect 1 dominates at smaller off-nadir angles, and thus the minimum reflectance occurs closer to nadir as supported by Figs. 3 and 5 and Ref. 2.

C. IR Band—Complete Canopy Cover

The reflectance distribution for the complete canopies in the IR band seems to follow similar trends as for complete canopies in the visible band[2,14] (Figs. 13, 14). However, there are exceptions. For example, the 0740 EST data for the soybean canopy show a minimum reflectance toward the backscatter direction rather than near nadir as is commonly the case for large solar zenith angles.

Extreme azimuthal variation is absent because the transmittance and reflectance of vegetation are nearly equal (Table II) as discussed above. In addition, the leaf reflectance in the IR is relatively high, and thus multiple scattering tends to make the distribution more azimuthally symmetric.[5] The strong backscattering characteristics of the soil (Fig. 17) does not strongly influence the reflectance distribution becasue of the complete canopy cover and low soil reflectance as compared with leaf reflectance.

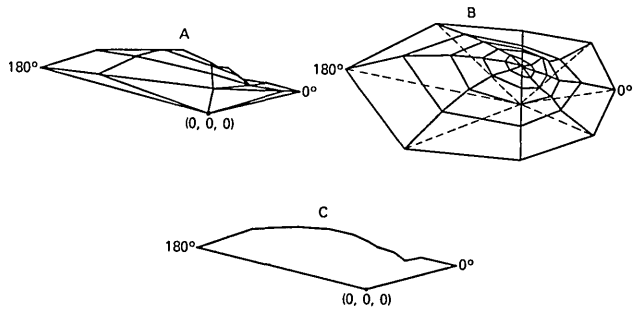

Figure 10. Three-dimensional plots of the directional reflectance in the visible band for the orchard grass at 0735 (EST). Symbols follow Fig. 2.

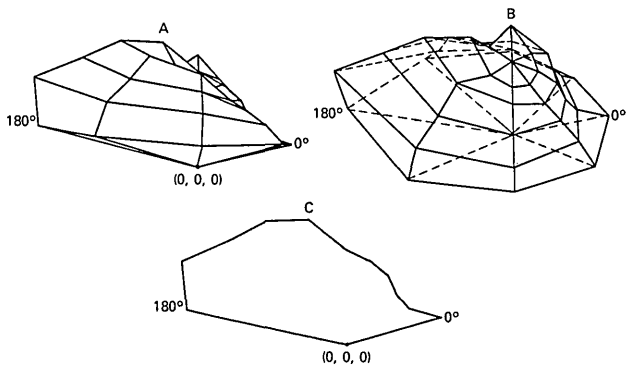

Figure 11. Three-dimensional reflectance in the visible band for the orchard grass at 1002 (EST). Symbols follow Fig. 2.

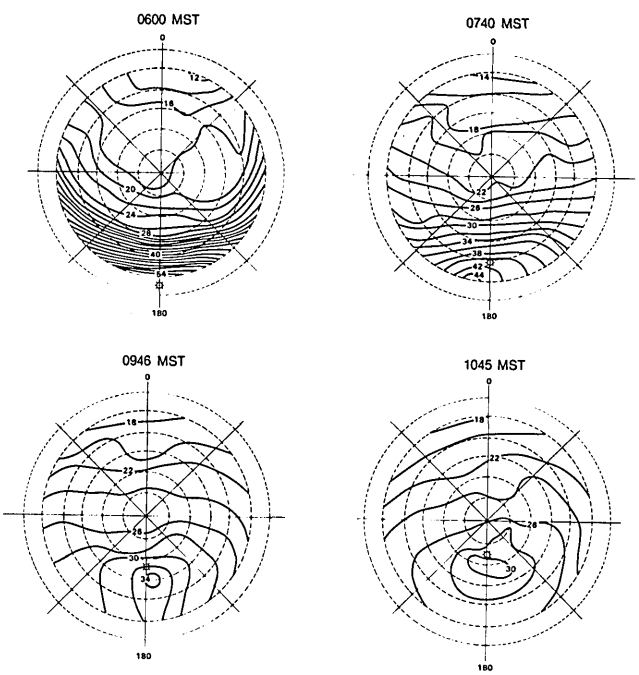

Figure 12. Polar plots of the directional reflectance (%) in the visible band for the bare soil. Symbols follow Fig. 3.

D. IR Band—Sparse Canopy Cover

In general, the soil reflectance in the IR is much lower than the leaf reflectance (Table II). The opposite situation exists for the visible band. As a consequence, we would expect the strong backscatter peak of soil to have much less effect on the directional reflectance in the IR band. Furthermore, the strong multiple scattering (diffuse radiation) in the IR band tends to further decrease azimuth variations in reflectance. For ex-

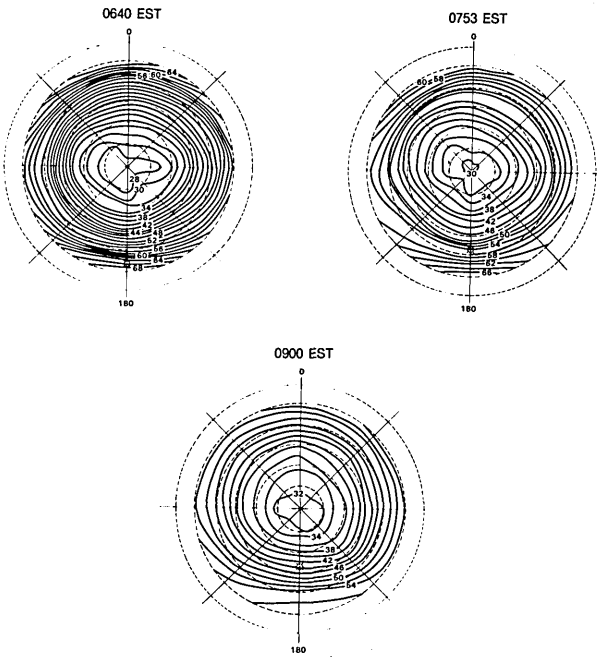

Figure 13. Polar plots of directional reflectance (%) in the IR band for the grass lawn. Symbols follow Fig. 3.

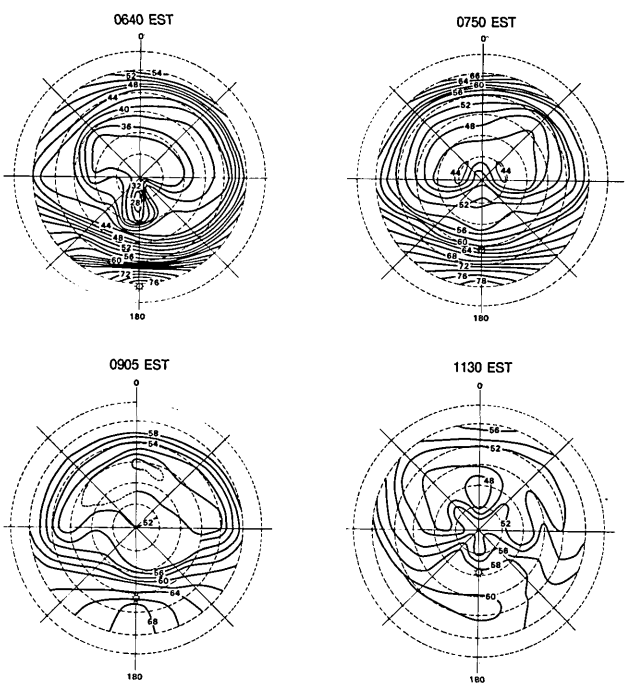

Figure 14. Polar plots of directional reflectance (%) in the IR band for the soybeans. Symbols follow Fig. 3.

ample, no strong backscattering from the soil is evident for the corn canopy with 25% cover (Fig. 15) or the alfalfa canopy (42% cover) as reported by Kirchner *et al.*[2] However, for more sparse canopies one would expect the backscatter peak to be more apparent, particularly for relatively small solar zenith angles.

In any azimuthal direction away from the point of minimum reflectance near nadir, the reflectance increases with increasing off-nadir sensor angle. Again, two mechanisms are operating as the off-nadir view angle increases: (1) the sensor views a higher proportion of the more reflective vegetation and a lower proportion of the less reflective soil, and (2) the sensor views a higher proportion of vegetation components in the upper layers of the canopy which scatter a higher proportion of solar incident flux (Effect 1).

The orchard grass (Fig. 16) and alfalfa[2] suggest that the point of minimum reflectance can shift from the nadir point at large solar zenith angles to more off-nadir in the forward scattering directions as the sun rises. These are the same trends as seen in the visible band, and the mechanisms are the same except that the effects of soil reflectance are less in the IR, because of the high leaf reflectance and transmittance, and low soil reflectance.

E. Further Discussion

For homogeneous scenes (e.g., no predominant row structure) there seems to be symmetry about the principal plane of the sun for all wavelengths. However, one would only expect such symmetry as long as the geometric structure was symmetric about the principal plane of the sun. That is, the leaf orientation distributions on each side of the principal plane must be mirror images of each other. For example, true diaheliotropic movements of leaves in a canopy would cause geometric symmetry about the principal plane (i.e., the plane defined by the nadir vector and the solar vector). However, any geometric asymmetry about the principal plane due to lagging diaheliotropic leaf movements, wind, or stress may cause asymmetric reflectances about the principal plane.[9] An extreme example of this asymmetric effect is in row crops as discussed in detail by Kimes *et al.*[19]

Validation of current radiative transfer models of vegetation canopies should be compared to directional radiometric measurements that cover the entire exitance hemisphere as measured in this study. Such rigorous tests are rare in the literature. However, from such tests it is readily apparent if a model is deficient and what improvements can be made.[5] For example, it is clear from this study that models must be able to handle the anisotropic scattering of the soil for sparse canopies.

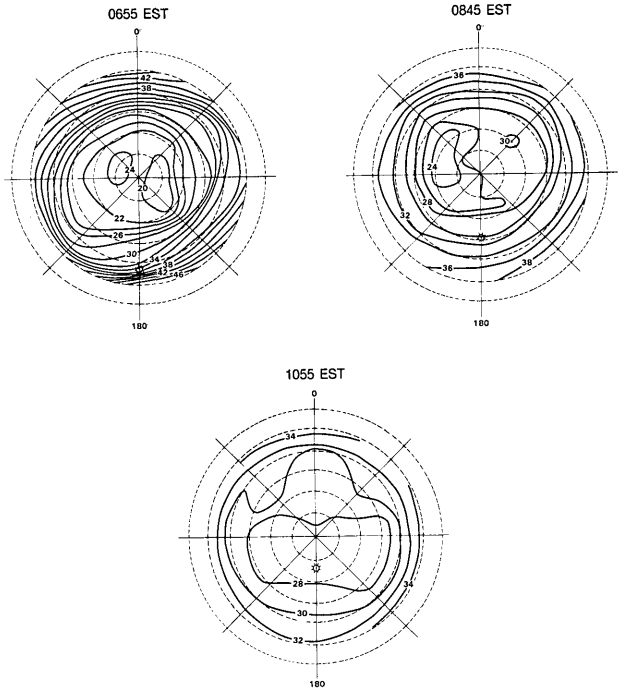

Figure 15. Polar plots of directional reflectance (%) in the IR band for the corn. Symbols follow Fig. 3.

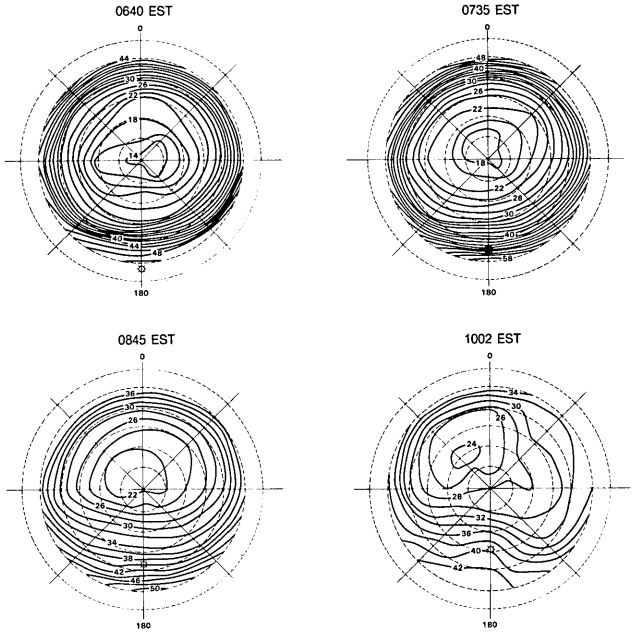

Figure 16. Polar plots of directional reflectance (%) in the IR band for the orchard grass. Symbols follow Fig. 3.

IV. Summary

The dynamics of directional reflectance factors of homogeneous vegetation canopies were observed, and underlying physical mechanisms were proposed which are supported by a number of field and modeling studies. The directional reflectance factor distribution changes significantly as a function of the geometric structure of the scene, solar zenith angle, and optical properties of the vegetation components and soil. The trends and magnitude of changes and the physical mechanisms causing them are important information in interpreting directional data from aircraft and satellite systems. Furthermore, the measured data and knowledge of the physical mechanisms of the observed

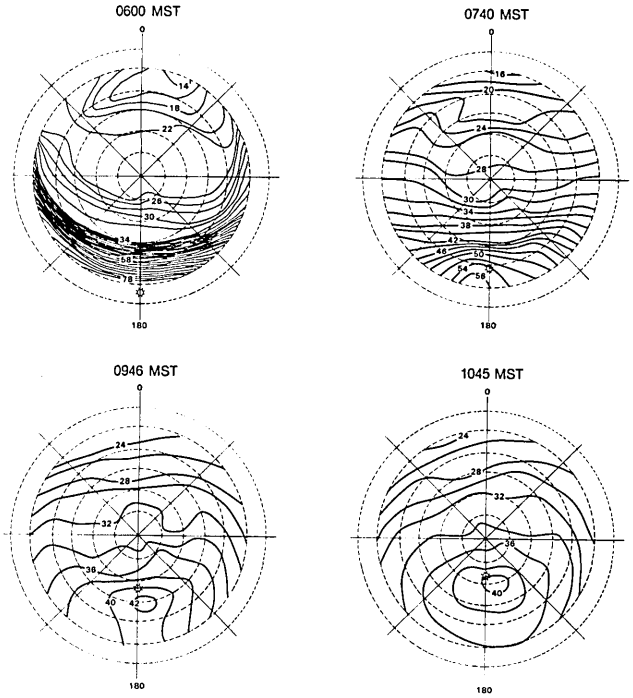

Figure 17. Polar plots of directional reflectance (%) in the IR band for the bare soil. Symbols follow Fig. 3.

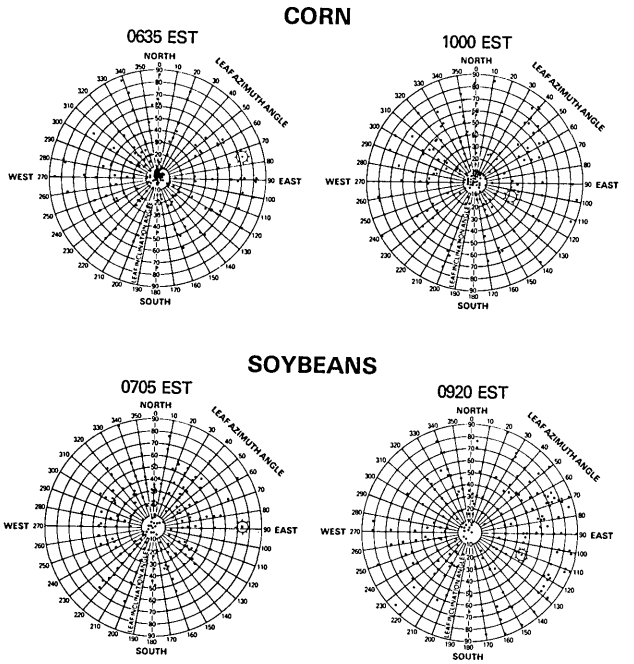

Figure 18. Leaf inclination–azimuth angle distribution of the corn and soybean canopies. Standard time of measurements is indicated.

dynamics of the data provide rigorous validation and verification tests for theoretical radiative transfer models. Finally, the data and knowledge of the physical mechanisms provide a sound basis for proposing quantitative techniques for extracting information of canopy features from directional radiometric data.

The author would like to thank Brent Holben and Wayne Newcomb for help in collecting field data, Jim Tucker for general support and loan of the 3-band hand-held radiometer, Rick Latty for his help and expertise in running his 3-D plotting programs for the MOVIE routine, Jim McMurtrey for providing various scenes at Beltsville, and Paul Pinter and Ray Jackson for providing soil plots in Phoenix, Ariz.

Appendix

The leaf inclination–azimuth angle distribution for the corn and soybean is shown in Fig. 18. Two angles were measured for each leaf sample: The inclination angle, which is equivalent to the zenith angle of the vector normal to the leaf's upper surface, and the azimuth angle, which is the azimuth direction of the vector normal to the leaf's upper surface. The azimuth angle is measured positive to the east from true north (0°). Leaves were randomly sampled from the upper third layer of the soybean canopy and the entire canopy of the corn.

References

1. D. S. Kimes, J. A. Smith, and K. J. Ranson, Photogramm. Eng. Remote Sensing **46**, 1563 (1980).
2. J. A. Kirchner, D. S. Kimes, and J. E. McMurtrey III, Appl. Opt. **21**, 3766 (1982).
3. C. J. Tucker, C. Vanpraet, E. Boerwinkle, and A. Gaston, Remote Sensing Environ. (1982), in press.
4. J. A. Kirchner and C. C. Schnetzler, Int. J. Remote Sensing **2**, 253 (1981).
5. D. S. Kimes and J. A. Kirchner, Appl. Opt. **21**, 4119 (1982).
6. D. S. Kimes and J. A. Kirchner, Remote Sensing Environ. **12**, 141 (1982).
7. J. V. Dave, Sol. Energy **21**, 361 (1978).
8. H. Christiansen and M. Stephenson, MOVIE, *BYU Training Manual, Civil Engineering* (Brigham Young U., Provo, Utah, 1982).
9. D. S. Kimes and J. A. Kirchner, Int. J. Remote Sensing (1982); accepted.
10. K. L. Coulson, Appl. Opt. **5**, 905 (1966).
11. F. D. Eaton and I. Dirmhirn, Appl. Opt. **18**, 994 (1979).
12. D. D. Egbert and F. T. Ulaby, Photogramm. Eng. **38**, 556 (1972).
13. K. T. Kriebel, Appl. Opt. **17**, 253 (1978).
14. K. J. Ranson, V. C. Vanderbilt, L. L. Biehl, B. F. Robinson, and M. E. Bauer, "Soybean Canopy Reflectance as a Function of View and Illumination Geometry," in *Proceedings, Fifteenth International Symposium on Remote Sensing of Environment* (Environmental Research Institute of Michigan, Ann Arbor, 1981).
15. R. E. Oliver and J. A. Smith, "A Stochastic Canopy Model of Diurnal Reflectance," Final Report, U.S. Army Research Office, Durham, N.C., DAH C04-74-60001 (1974). 105 pp.; T. Nilson. Agric. Meteorol. **8**, 25 (1971).
16. J. A. Smith and K. J. Ranson, "Bidirectional Reflectance Studies Literature Review," NASA/GSFC, prepared by ORI, Inc., 1400 Spring St., Silver Spring, Md. 20910 (1979).
17. G. H. Suits, Remote Sensing Environ. **2**, 175 (1972).
18. V. V. Salomonson and W. E. Marlatt, Remote Sensing Environ. **2**, 1 (1971).
19. D. S. Kimes, W. W. Newcomb, J. B. Schutt, P. J. Pinter, Jr., and R. D. Jackson, Int. J. Remote Sensing submitted.